Wave Propagation Characteristics and Electromagnetic Transient Analysis of Underground Cable Systems Considering Frequency-Dependent Soil Properties

Theofilos A. Papadopoulos, *Senior Member, IEEE*, Zacharias G. Datsios, *Member, IEEE*, Andreas I. Chrysochos, *Member, IEEE*, Pantelis N. Mikropoulos, *Senior Member, IEEE*, and Grigoris K. Papagiannis, *Senior Member, IEEE*

***Abstract*—The accurate estimation of the influence of the imperfect earth on the propagation characteristics of conductors is a crucial issue in electromagnetic (EM) transient analysis. In this aspect, the frequency-dependence of the soil electrical properties should be also considered. The effects of the dispersion of soil electrical properties on EM propagation have been investigated mostly for overhead transmission lines. This article presents a detailed EM transient analysis of underground cable systems taking into consideration the frequency-dependent (FD) soil properties. A generalized earth formulation of cable earth return impedance and shunt admittance is adopted. Propagation characteristics and transient responses are calculated by using both FD soil models and constant soil properties, as well as approximate earth formulations, neglecting the influence of the imperfect earth on shunt admittances; significant differences are observed. Guidelines for the accurate evaluation of earth conduction effects on the transient performance of underground cable systems are also introduced.**

***Index Terms*—Earth conduction effects, electromagnetic transients, frequency-dependent soil models, underground cables.**

I. Introduction

STUDIES of electromagnetic (EM) transients in power systems require the use of the accurate component models with their parameters calculated over a wide frequency range. Regarding underground cable systems, the first approach by Pollaczek [1] used formulas for the calculation of the cable impedances, assuming earth as a perfect conductor. Later, Sunde [2] included in Pollaczek's formulas the influence of earth permittivity. Pollaczek's formulation is implemented in the routines of most EM transient simulation software platforms. However, the accuracy of these pioneering approaches is limited to low-frequency applications (roughly up to some kHz), since both ignore the influence of the imperfect earth on the cable shunt admittance.

More recent approaches [3]–[6] propose earth models including earth correction terms for the shunt admittance of underground power cables. A systematic investigation using such models has been presented in [7]. However, in all the above models, the electrical properties of soil, namely conductivity, and permittivity, are considered constant, although it is well established that they are frequency-dependent (FD) [8]–[22].

FD soil electrical properties [8]–[20] have been included in several models, as summarized in [21] and [22]. Such models have been used for the analysis of the transient performance of overhead transmission lines [22]–[25] and grounding systems [21], [22], [26], [27] subjected to lightning surges, as well as for the evaluation of transient EM fields and induced voltages [19], [22], [28], [29]. However, the influence of FD soil characteristics on EM transient analysis of underground cable systems has not been thoroughly investigated [30]–[32].

This article presents an investigation on the effects of the frequency-dependence of the soil electrical properties on the propagation characteristics of multiconductor, underground cable systems; a preliminary analysis for the case of single conductor has been presented in [32]. A generalized earth formulation, as presented in [4], is adopted, considering earth conduction effects on both cable series impedances and shunt admittances. Several FD soil models are evaluated and further employed in the calculation of the propagation characteristics of underground cables. The latter are also calculated for constant soil properties, as well as by using the Sunde's approximate earth formulation. Results are compared and discussed also on the basis of EM transient responses. Guidelines for the investigation and accurate evaluation of earth conduction effects on the transient performance of underground cable systems are also introduced.

II. Earth Impedance and Admittance Parameters

We consider a case of two single-core cables buried in a homogeneous earth, as shown in Fig. 1. The influence of earth

Manuscript received December 22, 2019; revised March 7, 2020; accepted April 5, 2020. *(Corresponding author: Theofilos A. Papadopoulos.)*

Theofilos A. Papadopoulos is with Power Systems Laboratory, Department of Electrical and Computer Engineering, Democritus University of Thrace, 67100 Xanthi, Greece (e-mail: thpapad@ee.duth.gr).

Zacharias G. Datsios, Pantelis N. Mikropoulos, and Grigoris K. Papagiannis are with the School of Electrical and Computer Engineering, Aristotle University of Thessaloniki, 54124 Thessaloniki, Greece (e-mail: zdatsios@auth.gr; pnm@eng.auth.gr; grigoris@eng.auth.gr).

Andreas I. Chrysochos is with Cablel Hellenic Cables S.A., Maroussi, 15125 Athens, Greece (e-mail: achrysochos@fulgor.vionet.gr).

Color versions of one or more of the figures in this article are available online at http://ieeexplore.ieee.org.

Digital Object Identifier 10.1109/TEMC.2020.2986821

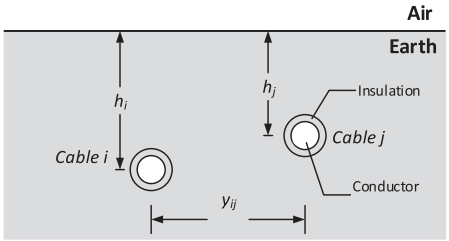

Fig. 1. Layout of two insulated underground conductors.

conduction effects on the per-unit-length parameters of the two cables is represented by means of the self and mutual earth impedance, Z'_e, and admittance, Y'_e, terms. The mutual terms are given in general form in (1) and (2), respectively [4].

$$Z'_e = \frac{j\omega\mu_1}{2\pi}\int_0^{+\infty} F_e(\lambda)\cos(y_{ij}\lambda)\,d\lambda \tag{1}$$

$$F_e(\lambda) = \frac{e^{-\alpha'_1|h_i-h_j|} - e^{-\alpha'_1(h_i+h_i)}}{\alpha'_1} + \frac{2\mu_0 e^{-\alpha'_1(h_i+h_j)}}{a'_1\mu_0 + a'_0\mu_1} \tag{2}$$

$$Y'_e = j\omega P_e^{-1} \tag{3}$$

$$P_e = \frac{j\omega}{2\pi(\sigma_1 + j\omega\varepsilon_1)}\int_0^{+\infty}[F_e(\lambda)+G_e(\lambda)]\cos(y_{ij}\lambda)\,d\lambda \tag{4}$$

$$G_e(\lambda) = \frac{2\mu_0\mu_1\alpha'_1\left(\gamma_1^2-\gamma_0^2\right)e^{-\alpha'_1(h_i+h_j)}}{(a'_1\mu_0+a'_0\mu_1)\left(a'_1\gamma_0^2\mu_1+a'_0\gamma_1^2\mu_0\right)} \tag{5}$$

where $a'_k = \sqrt{\lambda^2+\gamma_k^2+{k'_x}^2}$ and $k'_x = \omega\sqrt{\mu_1\varepsilon_1}$. The EM properties of air, i.e., permittivity, permeability and conductivity, are denoted as ε_0, μ_0, σ_0, respectively; σ_0 is equal to zero. Accordingly, the EM properties of earth are $\varepsilon_1 = \varepsilon_{r1}\varepsilon_0$, $\mu_1 = \mu_{r1}\mu_0$ and σ_1, where ε_{r1} is the relative permittivity and μ_{r1} the relative permeability of the earth. The corresponding propagation constants are:

$$\gamma_m = \sqrt{j\omega\mu_m(\sigma_m + j\omega\varepsilon_m)} \tag{6}$$

with the subscript *m* taking values 0 and 1 for air and earth, respectively. The self-parameters of cable *i* are derived by replacing h_j with h_i and y_{ij} with the cable outer radius.

III. Frequency-Dependent Behavior of Earth

Soil is a non-ferromagnetic dispersive lossy dielectric material ($\mu_{r1} \approx 1$). Therefore, it can be characterized by its FD electrical properties: relative permittivity ε_{r1} and conductivity σ_1. Its behavior can be described by means of three frequency regions by comparing the conduction ($J_c = \sigma_1 E$) and displacement ($J_d = \varepsilon_{r1}\varepsilon_0\omega E$) current densities. Note that E is the electric field propagating in soil. These regions are [7]:

1) *Low-frequency (LF) region:* The conduction current is predominant ($J_c >> J_d$), thus earth behaves as a conductor.
2) *Mid-frequency (MF) or intermediate region:* As frequency increases J_c and J_d become comparable; earth behaves both as conductor and insulator. The effect of J_d becomes more dominant for lower conductivity since J_c decreases; for such cases the MF region refers to lower frequencies.
3) *High-frequency (HF) region:* The displacement current dominates ($J_c << J_d$); earth behaves mainly as an insulator.

Where studying EM transients with frequency content up to a few MHz, the LF, and MF regions are relevant for common soils with LF conductivity higher than 0.001 S/m. The HF region is pertinent to higher frequencies or to lower conductivity soils.

A. Frequency-Dependent Soil Models

Several models are available for the prediction of the frequency-dependence of soil electrical properties applicable to switching and lightning transient studies (Appendix). These can be divided into soil models based on measurements performed on soil samples and undisturbed ground in the field.

1) Models Based on Soil Samples: The first soil model (S) was introduced by Scott *et al*. [8] in 1964 empirically derived from laboratory measurement results (10^2–10^6 Hz). It was later revised in 1966 [9], considering additional test data. The work of Scott *et al*. [8]–[10] formed the basis for the Longmire and Smith (LS) (10^2–$2\cdot10^8$ Hz) [11] and Messier (M) (10^2–10^6 Hz) [12], [13], [19], [20], [21] models. It is noteworthy that the LS model was verified using circuit analysis and considers also the higher-frequency laboratory measurements performed by Wilkenfeld [11].

Three soil models were proposed based on sets of test data on soil samples different than those of Scott *et al*. [8]–[10]: the Visacro and Portela (VP) [14], [21], Portela (POR) [15] and Datsios and Mikropoulos (DM) (Appendix) models. Visacro and Portela [14] performed laboratory tests on three soils with varying water content and introduced empirical expressions in the frequency range of 10^2–$2\cdot10^6$ Hz. The POR model [15] was developed considering measurements (10^2–$2\cdot10^6$ Hz) conducted on undisturbed soil samples from several regions in Brazil. The DM model was derived from the laboratory measurement results (42–10^6 Hz) reported in [18] for several sandy soils with variable water content (2.5% up to saturation), and was validated against literature data on similar soils.

2) Models Based on Field Tests: Visacro and Alipio introduced two FD soil models on the basis of field measurements at several areas in Brazil: VA [16] and AV [17] models (10^2–$4\cdot10^6$ Hz). Recently, CIGRE WG C4.33 [22] proposed different expressions for the same dataset.

3) Discussion on Models Based on Samples and Field Tests: Measurements on undisturbed or reconstituted soil samples yield the actual FD electrical properties for the soil under test. On the contrary, field measurements on undisturbed ground yield apparent electrical properties corresponding to the ground up to a certain depth depending on soil characteristics and conditions, electrode configuration and dimensions, as well as on the excitation frequency affecting the penetration depth. The effect of these influencing factors has not yet been fully investigated and clarified. This may influence considerably the interpretation of measurement results and the derivation of an appropriate soil model representing the actual ground; a preliminary account on this issue has been presented in [33].

TABLE I
PROPERTIES OF THE EXAMINED SOIL CASES

Case	σ_1 (S/m)	ε_{r1}
#A1	0.01	15
#A2	0.01	43
#A3	FD: 0.01 @ 100 Hz	FD
#B1	0.001	5
#B2	0.001	23
#B3	FD: 0.001 @ 100 Hz	FD

Another important aspect is the contact resistance and electrode polarization effects on measurement results. These are inherent in two- and three-electrode arrangements and may introduce considerable error. Apart from the POR model, which is derived from four-electrode tests, the remaining models were based on two- and three-electrode configurations introducing uncertainty to the experimental results. However, Scott *et al.* [8]–[10] performed an extensive investigation on minimizing electrode polarization effects and Datsios and Mikropoulos [18] introduced a method to determine the critical frequency above which such effects do not influence measurement results.

Based on the above, it can be concluded that all models have limitations; a thorough evaluation is required based on the physical processes involved.

4) Causality of Soil Models: Complex spectral data, such as those of soil electrical properties, must satisfy the Kramers-Kronig relations [19], [21] in order to ensure causality. This is the case for the soil properties predicted by the LS, M, POR, AV, and CIGRE FD soil models, yielding, therefore, causal solutions for EM transient problems. However, non-causal FD soil models are also appropriate for engineering applications, since, as observed for example from the simulation results presented in [19], [21], the error introduced is commonly limited to non-zero estimates for time instant $t = 0$ s; the latter are insignificant for engineering applications.

B. Examined Soil Cases

Table I shows the electrical properties of the investigated soils. In soil cases #A1 and #A2, σ_1 and ε_{r1} are assumed frequency independent; actually, $\sigma_{1,LF} = 0.01$ S/m, $\varepsilon_{r1} = 15$ and 43 for cases #A1 and #A2, respectively. The value of 15 can be considered as typical for $\sigma_{1,LF} = 0.01$ S/m [34], whereas that of 43 is calculated from the LS model, i.e., the most commonly adopted FD soil model, at 1 MHz. In soil case #A3, σ_1 and ε_{r1} are FD with $\sigma_{1,LF} = 0.01$ S/m at 100 Hz; the variation of σ_1 and ε_{r1} in the investigated frequency range of 1 kHz to 1 MHz can be estimated by applying the FD soil models of the Appendix. Soil cases #B1–#B3 are similar to #A1–#A3 with $\sigma_{1,LF} = 0.001$ S/m. It is important that the $\sigma_{1,LF}$ values of 0.01 S/m and 0.001 S/m were selected in order to consider the upper and lower limit of the soil conductivity range commonly found at underground cable systems installation sites; this is in line with previous studies [3], [6].

C. Comparison of Soil Properties

Fig. 2(a) and (b) shows σ_1 and ε_{r1}, respectively, as a function of frequency for the soil case #A3 considering the soil models of Section III.A (expressions in Appendix); the corresponding results for the soil case #B3 are presented in Fig. 2(c) and (d).

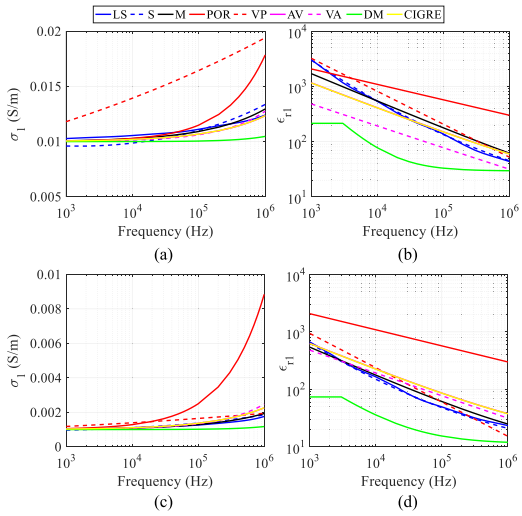

Fig. 2. Soil electrical properties. (a) σ_1, (b) ε_{r1} for soil case #A3 and (c) σ_1, (d) ε_{r1} for soil case #B3 calculated by all FD soil models.

As can be seen from Fig. 2(a) and (c), σ_1 increases with frequency for all FD soil models, especially when $\sigma_{1,LF}$ is 0.001 S/m. Thus, as $\sigma_{1,LF}$ decreases, the frequency-dependence of σ_1 becomes enhanced. Deviations in the σ_1 estimates among soil models generally decrease with decreasing $\sigma_{1,LF}$ and frequency; the most pronounced dependence of σ_1 on frequency is predicted by the POR and VP models whereas the less pronounced by the DM model. From Fig. 2(b) and (d) it is apparent that ε_{r1} decreases significantly with frequency, with the rate of decrease varying among models. The POR and VA models yield ε_{r1} estimates which are independent of $\sigma_{1,LF}$; this is in contrast with the behavior of actual soils as well as the predictions of the other soil models (lower ε_{r1} for lower soil conductivity).

For the examined soil cases #A3 and #B3, the predictions of the S, LS, M, AV and CIGRE soil models are generally comparable; deviations are observed in the VA and VP model predictions on ε_{r1} and σ_1, respectively. The DM model predictions deviate significantly (lower ε_{r1} and lower σ_1 values), since the model refers to sandy soils (low specific surface), where polarization and conduction phenomena are less marked [18]. The deviations among FD soil model predictions seen in Fig. 2 also stress the need for a thorough evaluation based on the physical behavior of actual soils.

Based on the above, in the next subsection the widely applied LS model as well as the POR and DM models are selected for investigating the propagation characteristics of underground cable systems. This selection is also based on the discussion of Section III.A and on the fact that these models may represent the widest variation of the soil electrical properties as predicted by FD soil models (see Fig. 2).

D. Comparison of Propagation Characteristics

The propagation characteristics of three identical single-core cables in flat formation are calculated via the methodology of [35] using the LS, POR and DM soil models (Appendix). As shown in Fig. 3, the cable system is buried 1 m under the ground

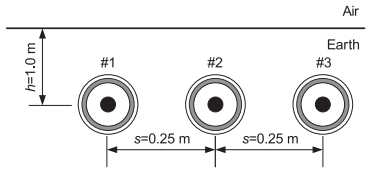

Fig. 3. Cable configuration under investigation.

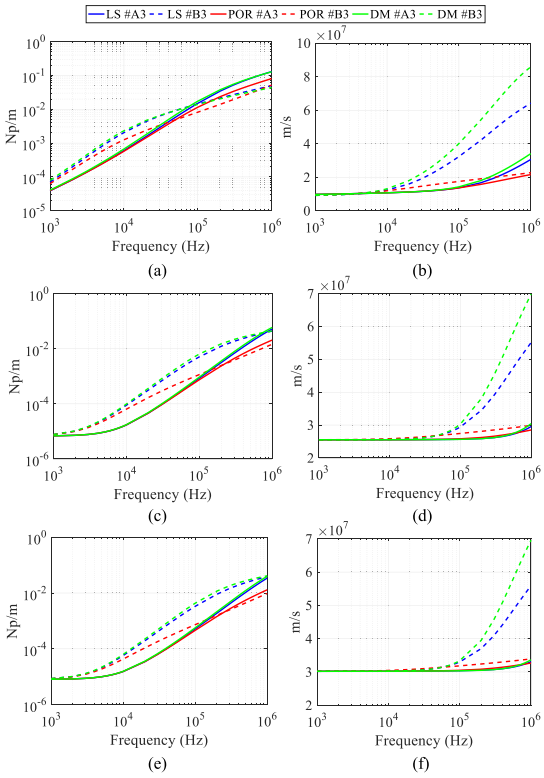

Fig. 4. Mode propagation characteristics: attenuation constant and velocity of (a), (b) ground mode and inter-sheath mode (c), (d) #1, (e), (f) #2.

surface with spacing $s = 0.25$ m; a detailed description of the investigated system has been given in [4].

In Fig. 4 the attenuation constant and velocity of the three (ground and the two inter-sheath modes #1 and #2) out of the six cable modes are compared for soil cases #A3 and #B3, using the LS, POR and DM models. These modes are mainly affected by soil properties [4], [6], since the ground mode expresses the influence of earth on the cable metallic parts and the inter-sheath modes the coupling between cables through earth.

Concerning mode attenuation constants (see Fig. 4), the LS and DM soil models yield generally similar results in the examined frequency range for both soil cases #A3 and #B3; this applies to all modes. The POR soil model results deviate for frequencies higher than ∼100 kHz for soil case #A3 and ∼10 kHz for soil case #B3. Regarding mode velocities (see Fig. 4), for soil case #A3, characterized by high $\sigma_{1,LF}$ value, a similar behavior among soil models is observed. This is not the case for the poorly conductive soil (case #B3), where significant differences are evident. The deviations in propagation characteristics among soil models become more marked with increasing frequency and decreasing $\sigma_{1,LF}$; this is associated with σ_1 and ε_{r1} variations (see Fig. 2), as well as with the more pronounced effects of

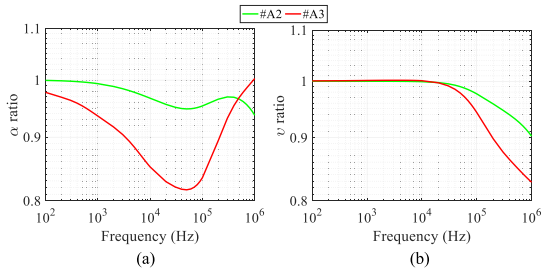

Fig. 5. Propagation characteristics ratios for soil cases #A2 and #A3. Ground mode (a) attenuation constant and (b) velocity.

displacement current on cable propagation characteristics with frequency.

In light of the above and by considering also that the DM soil model refers to sandy soils and that in the POR soil model ε_{r1} is taken independent of $\sigma_{1,LF}$, the LS soil model is adopted hereafter for the analysis of EM field propagation in underground cables.

IV. FD Soil Properties Effects on Cable Propagation Characteristics

To demonstrate the impact of the frequency-dependence of soil electrical properties on cable propagation characteristics, comparisons are carried out using the soil cases of Table I. For this purpose, the following ratio is employed for the ground and the inter-sheath cable modes:

$$\text{ratio}\,(f) = \frac{|\text{propagation chararacterstics}_{\text{FD}}\,(f)|}{|\text{propagation chararacterstics}_{\text{constant}}\,(f)|}. \qquad (7)$$

In the denominator of (7) soil cases #A1 and #B1 are assumed as reference, since they represent the most commonly adopted soil models. The numerator includes soil cases #A2 and #B2 as well as #A3 and #B3, using the LS formulation.

A. Earth Formulation Including Earth Admittance

In Fig. 5 the ground mode attenuation constant and velocity ratios are compared for soil cases #A2 and #A3. It is shown that both propagation characteristics results are generally similar for soil cases #A1 and #A2, presenting deviations lower than 10%. This is attributed to the fact that the examined soil cases in Fig. 5 are highly conductive ($\sigma_{1,LF} = 0.01$ S/m), thus the effects of ε_{r1} on cable propagation characteristics are minimal. However, for soil case #A3, significant differences are observed, especially for the mode attenuation constant for frequencies higher than some kHz mainly due to the FD behavior of σ_1. Differences are also observed in mode velocity, though for frequencies higher than ∼200 kHz. The differences between the results of soil cases #A2 and #A3 are mainly due to the FD σ_1 for soil case #A3 (for soil case #A2 $\sigma_1 = $ ct).

In Fig. 6 ground mode ratios as in Fig. 5 are presented for soil cases #B1–#B3. The corresponding results for the inter-sheath mode #1 are also plotted in Fig. 7. Differences in the ground mode propagation characteristics are more pronounced for these soil cases, compared to Fig. 5, due to the increased dependence of σ_1 on frequency and the increased effect of J_d. For frequencies

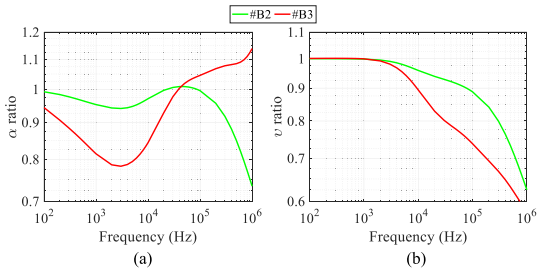

Fig. 6. Propagation characteristics ratios for soil cases #B2 and #B3. Ground mode (a) attenuation constant and (b) velocity.

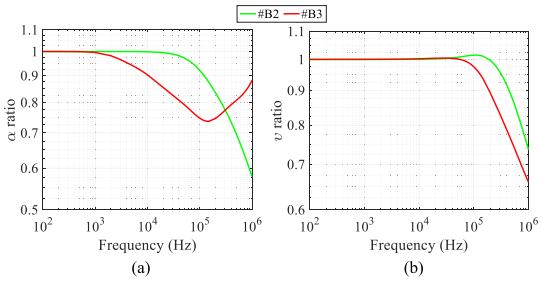

Fig. 7. Propagation characteristics ratios for soil cases #B2 and #B3. Inter-sheath mode #1 (a) attenuation constant and (b) velocity.

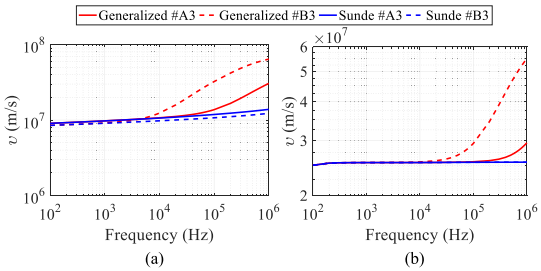

Fig. 8. Comparison of (a) ground mode and (b) inter-sheath mode #1 velocities for different earth approaches.

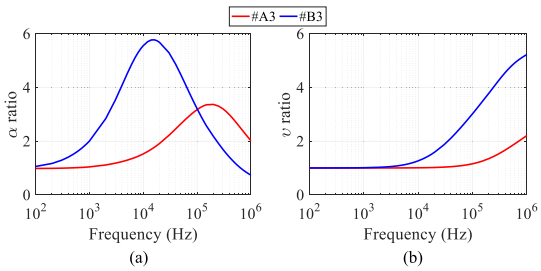

Fig. 9. Comparison of ratios for the ground mode (a) attenuation constant and (b) velocity between the generalized and approximate earth formulations.

above some kHz, the inter-sheath mode #1 propagation characteristics between soil cases #B3 and #B2 to #B1 present also significant differences.

The results of Figs. 5–7 can be analyzed, taking into consideration the increasing effect of J_d with frequency to the EM propagation involved in the cable outer insulation and thus to the ground and inter-sheath modes [6]. As a result of the higher ε_{r1}, in soil cases #A2 and #B2 the mode velocities are lower than soil cases #A1 and #B1. Additionally, due to the increase of σ_1 with frequency, the mode velocity becomes even lower for soil cases #A3 and #B3. As frequency increases and the effect of J_d becomes important, the total cable admittance is gradually determined by the earth admittance compared to the cable insulation [6], [7], [34]. Therefore, as the cable admittance becomes almost directly related to the soil EM properties and due to the significant increase of σ_1 at higher frequencies, the mode attenuation constant is higher for soil cases #B3 and #A3 than cases #B2 and #A2, respectively.

B. Effect of Earth Formulation

The effect of the soil FD dispersion on the propagation characteristics is further analyzed, by comparing results obtained by the generalized and the approximate earth formulation of Sunde [2]. Sunde's earth approach is typically considered in transient simulation programs and is derived assuming $k'_x = 0$ in (1)–(5) and most importantly a perfectly conducting earth by neglecting earth admittance of (3) [2].

The calculated ground and inter-sheath mode #1 velocity for the two earth approaches is compared in Fig. 8(a) and (b), respectively, for soil cases #A3 and #B3. Results obtained with the generalized formulation are affected by the FD behavior of earth. On the contrary, following Sunde's approach that considers earth as a perfect conductor (thus earth acts practically as an outer shield to the cable), the inter-sheath mode #1 behavior is exclusively determined by the EM characteristics of the cable outer sheaths. However, this assumption is only valid in the LF range as also results verify. Moreover, it is evident that the propagation characteristics obtained by the generalized formulation are sensitive to soil FD dispersion; this is mostly attributed to the influence of the earth admittance, as can be deduced by (3), where a direct relation of earth admittance and earth electrical properties is realized. However, this is not the case when the approximate earth formulation of Sunde is employed, since in the examined frequency range similar results for the different soil cases are obtained.

In Fig. 9(a) and (b) the ratios of (7) are plotted, assuming in the denominator the cable propagation characteristics using Sunde's earth formulation. It can be seen that the ground mode attenuation constant between the two approaches presents significant differences, starting at 2 kHz for soil case #A3 and 0.2 kHz for soil case #B3. The differences at low frequencies, where earth behaves mainly as a conductor, are attributed to the influence of J_c on the cable sheath self-conductance and on the mutual conductance between them (G_{ij}). As frequency increases, differences are also due to the increasing influence of J_d on the corresponding self and mutual cable sheath capacitances (C_{ij}) [6], [7]; this is most evident in the mode velocity results.

V. Transient Responses

To demonstrate the effects of soil modeling on cable transient responses, a voltage source producing a 1.2/50 μs double-exponential waveform of 1 pu amplitude is applied at the cable #1 core sending end of Fig. 3, with the receiving end open. The remaining cable cores, i.e., #2 and #3, are assumed open-ended at both ends. Single-point bonding is applied at cable sheaths with ground resistance 1 Ω at the sending end. The transient responses are obtained for different cable lengths

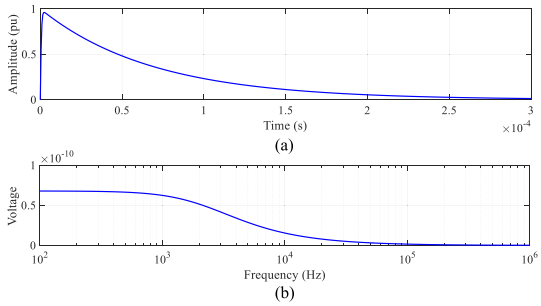

Fig. 10. Applied lightning impulse waveform at the sending end of the cable conductor: (a) response and (b) spectrum.

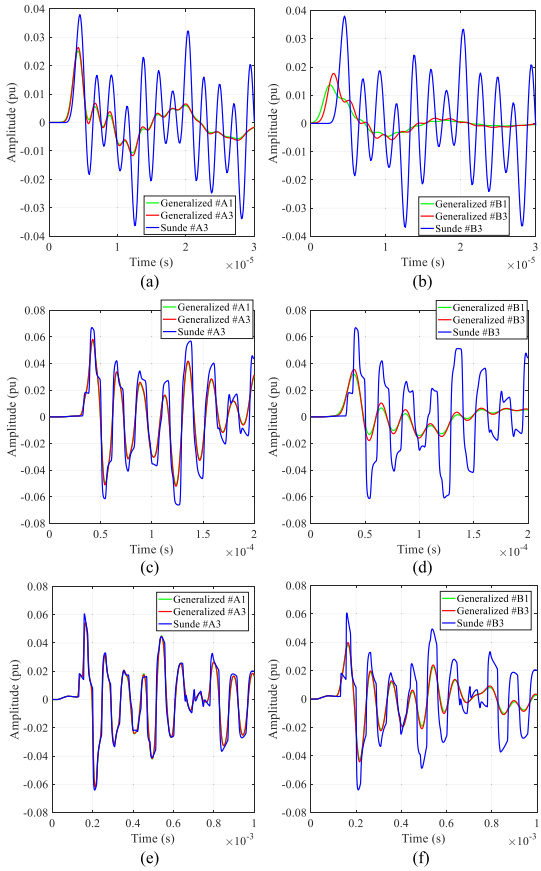

Fig. 11. Transient responses at end R of cable #1 sheath for $\ell = 100$ m and (a) $\sigma_{1,LF} = 0.01$ S/m, (b) $\sigma_{1,LF} = 0.001$ S/m, for $\ell = 1000$ m and (c) $\sigma_{1,LF} = 0.01$ S/m, (d) $\sigma_{1,LF} = 0.001$ S/m, for $\ell = 4000$ m and (e) $\sigma_{1,LF} = 0.01$ S/m, (f) $\sigma_{1,LF} = 0.001$ S/m.

by using the transient simulation model introduced in [36]. In Fig. 10 the applied voltage time-domain waveform and spectrum (calculated using the numerical Laplace transform) are presented.

In Fig. 11 the voltages at the cable #1 sheath receiving end are summarized for soil cases #A1, #A3 ($\sigma_{1,LF} = 0.01$ S/m) as well as for soil cases #B1 and #B3 ($\sigma_{1,LF} = 0.001$ S/m), assuming cable lengths $\ell = 100$, 1000, and 4000 m. The transient responses are simulated following three earth approaches. In the first two, the generalized earth formulation is applied. In the first approach, the soil properties are taken constant: soil cases #A1 and #B1 are examined. In the second approach, soil

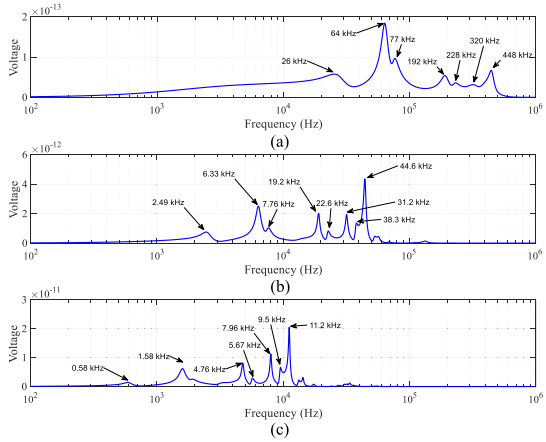

Fig. 12. Spectrum of transient response for cable length: (a) 100 m, (b) 1000 m, and (c) 4000 m, using the generalized approach and soil case #A3.

properties are assumed FD according to the LS soil model, thus soil cases #A3 and #B3 apply. It is evident that the comparison of the results between these two approaches reveals the effect of the adopted soil model on the transient responses. The third approach refers to Sunde's earth formulation and soil cases #A3 and #B3; direct comparisons of the so obtained results with those of the generalized approach are used for assessing the influence of the earth admittance term on cable propagation characteristics.

Deviations in the transient response of the cable system among the three approaches, in terms of voltage amplitude, attenuation rate and travel time, are evident in Fig. 11. This is more obvious for poorly conductive soils and for short cables. However, significant differences between the generalized and Sunde's approaches are observed even for long cable lengths (Fig. 11(d) and (f)). Since the generalized earth formulation takes into account the earth admittance in cable parameters, the transient response obtained shows a faster attenuation rate [higher mode attenuation constant, Fig. 9(a)] and travel time [higher mode velocity, Fig. 9(b)].

Generally, results reveal that the differences in the waveforms between the three earth approaches become more pronounced as the cable length decreases. This is substantiated by transient response spectrum analysis. Actually, in Fig. 12 the spectra of the transient responses of Fig. 11 referring to the generalized approach and soil case #A3 are shown. Evidently, as the cable length decreases, the frequency context of the transient response shifts gradually to higher frequencies, where differences in the propagation characteristics between soil models and earth approaches are enhanced. It is important that the transient response spectrum can be directly related to the resonance frequencies (RFs), characteristic of the cable configuration (linear time-invariant system). Therefore, the RFs affect the source waveform of Fig. 10 (system input) and determine accordingly the transient response at the cable end (system output). The RFs of an open-ended line can be determined in the modal domain as [37]:

$$f_{0,r}^{n} = \{1, 3, 5, \ldots\} \cdot f_{0,r} \tag{8}$$

TABLE II
RESONANT FREQUENCIES (KHZ)

Cable length (m)	RF order	Cable modes: ground ($r = 0$)	Inter-sheath #1 ($r = 1$)	Inter-sheath #2 ($r = 2$)
100	$n = 1$	28.70	64.05	75.86
	$n = 3$	86.10	192.14	227.59
	$n = 5$	143.51	320.23	379.32
	$n = 7$	200.91	448.32	531.04
1000	$n = 1$	2.52	6.38	7.55
	$n = 3$	7.95	19.16	22.69
	$n = 5$	13.62	31.96	37.86
	$n = 7$	17.67	44.67	52.88
4000	$n = 1$	0.60	1.60	1.89
	$n = 3$	1.87	4.79	5.67
	$n = 5$	3.18	7.98	9.44
	$n = 7$	4.19	11.17	13.21

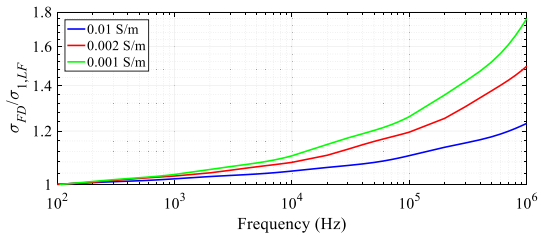

Fig. 13. Plot of $\sigma_{FD}/\sigma_{1,LF}$ against frequency for different soils; σ_{FD} according to the LS soil model.

where r is the mode index and $f_{0,r}$ is the frequency of the quarter-wavelength for each mode. For short-circuited lines even multiples of $f_{0,i}$ are considered [37].

Table II summarizes the RF values of the examined cable configurations for $n = 1$ to $n = 7$ using the generalized approach for soil case #A3. By comparing these values with those corresponding to the spectrum peaks of Fig. 12, it can be seen that the ground mode 1st RF as well as the 1st and the higher-order RFs of the two inter-sheath modes are directly related to the peaks of the corresponding spectrum. Therefore, the mode RFs calculated according to [37] can be used to evaluate the transient response spectrum of a cable system.

It should be noted that the findings of the present analysis can be considered as generalized; they were found to apply also for the cases of vertical and trefoil cable arrangements.

VI. GUIDELINES FOR SELECTING A VALID APPROACH FOR TRANSIENT ANALYSIS OF UNDERGROUND CABLE SYSTEMS

The effects of the FD soil electrical properties on the propagation characteristics and transient responses of underground single-core cable systems have been investigated, assuming FD and constant soil models as well as two earth formulation approaches. From the obtained results, these effects can be evaluated using three frequency criteria, namely f_{c1}, $f_{c2,}$ and f_{c3}.

The first frequency criterion (f_{c1}) is related to soil modeling. Using an FD soil model instead of one with constant soil properties affects considerably the calculated cable propagation characteristics, mainly due to the σ_1 dispersion especially as $\sigma_{1,LF}$ decreases. This effect can be accounted for by using the ratio $\sigma_{FD}/\sigma_{1,LF}$; note that σ_{FD} is the FD conductivity predicted by the soil model. Fig. 13 shows the variation of $\sigma_{FD}/\sigma_{1,LF}$ with frequency considering σ_{FD} according to the LS soil model and for several values of $\sigma_{1,LF}$. Deviations in $\sigma_{FD}/\sigma_{1,LF}$ higher than say 10%, may indicate the frequency boundary, f_{c1}, above which the frequency-dependence of soil properties should be taken into account. For frequencies higher than f_{c1} FD soil properties affect significantly cable propagation characteristics, especially the ground mode attenuation constant.

The second frequency criterion (f_{c2}) is related to earth formulation. The cable propagation characteristics obtained using the generalized formulation, which considers both earth series impedance and shunt admittance, differ from those obtained by Sunde's approximate earth formulation. This is attributed to the influence of J_c on cable earth conductance, as well as to an increasing influence of J_d with frequency on the cable shunt capacitances. A criterion for the determination of the frequency boundary, above which the generalized formulation should be considered, has been proposed in [7]. However, this criterion assumes constant soil properties. Where FD soil properties are considered a similar criterion is difficult to be derived. Thus, f_{c2} is empirically determined based on the conducted analysis. According to the present results, f_{c2} may range from some hundreds of Hz for cases of poorly conductive soils (around 0.001 S/m) to some tens of kHz for highly conductive soils (around 0.01 S/m).

Criteria f_{c1} and f_{c2} set the lower frequency limits above which FD soil models and the generalized earth formulation should be used. However, their influence on transient responses becomes less marked as the cable length increases; this, in terms of spectrum characterization, can be related to an upper-frequency boundary f_{c3}. The latter is realized as the 1st order cable RF of the ground mode, which is the lowest RF of all cable propagation modes. f_{c3} is influenced by earth conduction effects and also determines the lower limit of the frequency context of the transient response. When the calculated f_{c3} is higher than f_{c2} the generalized earth formulation should be applied for the transient analysis of the case under study. Additionally, FD soil modeling should be considered when f_{c3} is higher than f_{c1}.

VII. CONCLUSION

The effects of the frequency-dependence of soil electrical properties on the propagation characteristics and on the transient response of underground single-core cable systems have been investigated. Sunde's approximate earth formulation as well as a generalized one, considering both earth series impedance and shunt admittance have been applied.

First, several FD soil models have been examined, showing differences in the predicted behavior of the soil. Generally, divergence in the conductivity values is more marked for soils of lower low-frequency conductivity $\sigma_{1,LF}$; such soils exhibit lower permittivity values as well. Then, the propagation characteristics of the cable system have been evaluated by using soil models representing the full variation of the soil properties with frequency. In addition, soils with constant electrical properties have been considered. Differences in the propagation characteristics among the soil models are considerable, especially with decreasing $\sigma_{1,LF}$ and increasing frequency. This is

mainly attributed to the enhanced effects of σ_1 dispersion and displacement current.

The cable propagation characteristics, calculated using Sunde's approximate earth formulation, show low sensitivity to the dispersion of the soil electrical properties. This is not the case for the generalized formulation, which yields cable propagation characteristics sensitive to FD soil properties. Differences between the two earth approaches, resulting mainly from the omission of the earth admittance in Sunde's earth formulation, become more evident with increasing frequency.

Cable transient responses differ significantly for the different earth approaches, especially for poorly conductive soil and shorter cable lengths. The latter is related to the higher cable resonant frequencies (corresponding to the ground and inter-sheath cable modes), leading to higher frequency components in the transient response as also verified through spectrum analysis.

Guidelines for selecting a valid approach for EM transient analysis of underground cable systems have been introduced. The guidelines are based on three critical frequencies, used as criteria for assessing the necessity to use the generalized earth formulation as well as the FD soil modeling in transient analysis of underground cable systems.

Concurrent measurements of electromagnetic transients on underground cable systems and soil electrical properties would certainly contribute to the better understanding of the involved frequency-dependent effects.

APPENDIX

TABLE III
FREQUENCY-DEPENDENT SOIL MODELS

Model	Expressions	Parameters	Frequency range	Origin
Scott et al. [9] (S)	$\varepsilon_{r1}(f)=10^{D_1}$, $D_1=5.491+0.946\cdot\log_{10}\sigma_{1,LF}-1.097\cdot\log_{10}f+0.069\cdot(\log_{10}\sigma_{1,LF})^2-0.114\cdot\log_{10}\sigma_{1,LF}\log_{10}f+0.067\cdot(\log_{10}f)^2$ $\sigma_1(f)=10^{D_2}$, $D_2=0.028+1.098\cdot\log_{10}\sigma_{1,LF}-0.068\cdot\log_{10}f+0.036\cdot(\log_{10}\sigma_{1,LF})^2-0.046\cdot\log_{10}\sigma_{1,LF}\log_{10}f+0.018\cdot(\log_{10}f)^2$	σ_1 and $\sigma_{1,LF}$ in mS/m	10^2–10^6 Hz	Soil samples
Longmire and Smith [11] (LS)	$\varepsilon_{r1}(f)=\varepsilon_{r1,\infty}+\sum_{n=1}^{13}\frac{a_n}{1+(f/f_n)^2}$ $\sigma_1(f)=\sigma_{1,DC}+2\pi f\varepsilon_0\sum_{n=1}^{13}\frac{a_n f/f_n}{1+(f/f_n)^2}$ $f_n=10^{n-1}(125\sigma_{1,DC})^{0.8312}$ [21]	σ_1 and $\sigma_{1,DC}$ in S/m $\varepsilon_{r1,\infty}=5$ [11] a_n (pu) values listed in Table 1 of [11]	10^2–$2\cdot10^8$ Hz	Soil samples
Messier [12], [13] (extracted from [19]-[21]) (M)	$\varepsilon_{r1}(f)=\varepsilon_{r1,\infty}+\sqrt{\sigma_{1,DC}\varepsilon_{r1,\infty}/\pi f\varepsilon_0}$ $\sigma_1(f)=\sigma_{1,DC}+\sqrt{4\pi f\sigma_{1,DC}\varepsilon_0\varepsilon_{r1,\infty}}$	σ_1 and $\sigma_{1,DC}$ in S/m $\varepsilon_{r1,\infty}=8$ [21]	10^2–10^6 Hz	Soil samples
Visacro and Portela [14] (extracted from [21]) (VP)	$\varepsilon_{r1}(f)=2.34\cdot10^6\sigma_{1,LF}^{0.535}f^{-0.597}$ $\sigma_1(f)=\sigma_{1,LF}(f/100)^{0.072}$	σ_1 and $\sigma_{1,LF}$ in S/m	10^2–$2\cdot10^6$ Hz	Soil samples
Portela [15] (POR)	$\varepsilon_{r1}(f)=\beta_P\tan(\pi a_P/2)\cdot10^{-6}\cdot(2\pi f)^{a_P-1}/\varepsilon_0$ $\sigma_1(f)=\left[\sigma_{1,LF}+\beta_P(2\pi f)^{a_P}\right]\cdot10^{-6}$	σ_1 in S/m $\sigma_{1,LF}$ in μS/m In this work: $a_P=0.72$ pu $\beta_P=0.1$ s$^{0.72}$μS/m	10^2–$2\cdot10^6$ Hz	Soil samples
Datsios and Mikropoulos based on test results of [18] (DM)	$\varepsilon_{r1}(f)=1.24\sigma_{1,LF}^{0.415}\varepsilon_{r1,\infty}+(3000/f)^K\cdot\left[4\sigma_{1,LF}^{0.463}(2.9\varepsilon_{r1,\infty}-3.8)-1.24\sigma_{1,LF}^{0.415}\varepsilon_{r1,\infty}\right]$ $f\geq3$ kHz $\varepsilon_{r1}(f)=\varepsilon_{r1,3kHz}$ $f<3$ kHz due to electrode polarization effects $\sigma_1(f)=f\cdot10^{-6}(\sigma_{1,LF}+0.65\sigma_{1,LF}^{0.43})+[42-42(f-42)\cdot10^{-6}]\cdot[(\sigma_{1,LF}/42)-(\sigma_{1,LF}+0.65\sigma_{1,LF}^{0.43})\cdot10^{-6}]$ $K=0.537\sigma_{1,LF}^{0.16}$	σ_1 and $\sigma_{1,LF}$ in μS/cm $\varepsilon_{r1,\infty}$ corresponds to dry soil at 1 MHz $\varepsilon_{r1,\infty}=3.5$	42–10^6 Hz	Soil samples
Visacro and Alipio [16] (VA)	$\varepsilon_{r1}(f)=1.3+7.6\cdot10^3f^{-0.4}$ $f\geq10$ kHz $\varepsilon_{r1}(f)=\varepsilon_{r1,10kHz}$ $f<10$ kHz $\sigma_1(f)=\sigma_{1,LF}+1.2\cdot10^{-6}\sigma_{1,LF}^{0.27}(f-100)^{0.65}$	σ_1 and $\sigma_{1,LF}$ in S/m	10^2–$4\cdot10^6$ Hz	Field tests
Alipio and Visacro [17] (AV)	$\varepsilon_{r1}(f)=\varepsilon_{r1,\infty}+\frac{1.26\cdot10^{-3}\tan(\pi\gamma_{AV}/2)\sigma_{1,LF}^{0.27}f^{\gamma_{AV}-1}}{2\pi\varepsilon_0\cdot10^{6\gamma_{AV}}}$ $\sigma_1(f)=\left[\sigma_{1,LF}+1.26\,\sigma_{1,LF}^{0.27}(f/10^6)^{\gamma_{AV}}\right]\cdot10^{-3}$	σ_1 in S/m $\sigma_{1,LF}$ in mS/m $\varepsilon_{r1,\infty}=12$ [17] $\gamma_{AV}=0.54$ pu [17]	10^2–$4\cdot10^6$ Hz	Field tests
CIGRE WG C4.33 [22] (CIGRE)	$\varepsilon_{r1}(f)=12+9.5\cdot10^4\sigma_{1,LF}^{0.27}f^{-0.46}$ $\sigma_1(f)=\sigma_{1,LF}+4.7\cdot10^{-6}\sigma_{1,LF}^{0.27}f^{0.54}$	σ_1 and $\sigma_{1,LF}$ in S/m	10^2–$4\cdot10^6$ Hz	Field tests

where σ_1 is the soil conductivity, ε_{r1} is the relative permittivity of soil, f (Hz) is the frequency, $\sigma_{1,LF}$ is the soil conductivity at 100 Hz, $\sigma_{1,DC}$ is the DC soil conductivity, $\varepsilon_{r1,\infty}$ is the HF relative permittivity of soil

REFERENCES

[1] F. Pollaczek, "Über das Feld einer unendlich langen wechselstromdurchflossenen Einfachleitung," (in German), *Elektr. Nachr. Technik*, vol. 3, no. 4, pp. 339–359, 1926.

[2] E. D. Sunde, *Earth Conduction Effects in Transmission Systems*, 2nd ed., New York, NY, USA: Dover Publications, 1968, pp. 99–139.

[3] E. Petrache, F. Rachidi, M. Paolone, C. A. Nucci, V. A. Rakov, and M. A. Uman, "Lightning induced disturbances in buried cables-Part I: Theory," *IEEE Trans. Electromagn. Compat.*, vol. 47, no. 3, pp. 498–508, Aug. 2005.

[4] T. A. Papadopoulos, D. A. Tsiamitros, and G. K. Papagiannis, "Impedances and admittances of underground cables for the homogeneous earth case," *IEEE Trans. Power Del.*, vol. 25, no. 2, pp. 961–969, Apr. 2010.

[5] A. P. C. Magalhães, M. T. C. de Barros, and A. C. S. Lima, "Earth return admittance effect on underground cable system modeling," *IEEE Trans. Power Del.*, vol. 33, no. 2, pp. 662–670, Apr. 2018.

[6] H. Xue, A. Ametani, J. Mahseredjian, and I. Kocar, "Generalized formulation of earth-return impedance/admittance and surge analysis on underground cables," *IEEE Trans. Power Del.*, vol. 33, no. 6, pp. 2654–2663, Dec. 2018.

[7] T. A. Papadopoulos, A. I. Chrysochos, and G. K. Papagiannis, "Analytical study of the frequency-dependent earth conduction effects on underground power cables," *IET Gener. Transm. Distrib.*, vol. 7, no. 3, pp. 276–287, Mar. 2013.

[8] J. H. Scott, R. D. Carroll, and D. R. Cunningham, "Dielectric constant and electrical conductivity of moist rock from laboratory measurements," Sensor and Simulation Note 116, Tech. Letter, Special Projects-12, Geological Survey, U.S. Dep. of the Interior, Federal Center, Denver, CO, Aug. 1964.

[9] J. H. Scott, "Electrical and magnetic properties of rock and soil," Theoretical Notes, Note 18, Special Projects-16, Geological Survey, U.S. Dept. Interior, Federal Center, Denver, CO, May 1966.

[10] J. H. Scott, R. D. Carroll, and D. R. Cunningham, "Dielectric constant and electrical conductivity measurements of moist rock: A new laboratory method," *J. Geophys. Res.*, vol. 72, no. 20, pp. 5101–5115, Oct. 1967.

[11] C. L. Longmire and K. S. Smith, "A universal impedance for soils," DNA 3788T, Mission Research Corp., Santa Barbara, CA, Oct. 1975.

[12] M. A. Messier, "The propagation of an electromagnetic impulse through soil: Influence of frequency dependent parameters," Mission Research Corp., Santa Barbara, CA, USA, Tech. Rep. MRC-N-415, Feb. 1980.

[13] M. A. Messier, "Another soil conductivity model," JAYCOR, San Diego, CA, USA, Internal Rep., Jun. 1985.

[14] S. Visacro and C. M. Portela, "Soil permittivity and conductivity behavior on frequency range of transient phenomena in electric power systems," in *Proc. ISH*, Braunsweig, Germany, 1987, Art. no. 99.06.

[15] C. Portela, "Measurement and modeling of soil electromagnetic behavior," in *Proc. Int. Symp. EMC*, Seattle, WA, USA, Aug. 1999, vol. 2, pp. 1004–1009.

[16] S. Visacro and R. Alipio, "Frequency dependence of soil parameters: Experimental results, predicting formula and influence on the lightning response of grounding electrodes," *IEEE Trans. Power Del.*, vol. 27, no. 4, pp. 927–935, Apr. 2012.

[17] R. Alipio and S. Visacro, "Modeling the frequency dependence of electrical parameters of soil," *IEEE Trans. Electromagn. Compat*, vol. 56, no. 5, pp. 1163–1171, Oct. 2014.

[18] Z. G. Datsios and P. N. Mikropoulos, "Characterization of the frequency dependence of the electrical properties of sandy soil with variable grain size and water content," *IEEE Trans. Dielect. Elect. Insul.*, vol. 26, no. 3, pp. 904–912, Jun. 2019.

[19] F. M. Tesche, "On the modeling and representation of a lossy earth for transient electromagnetic field calculations," EMConsultant, Saluda, NC, Theoretical Notes, Note 367, Jul. 2002.

[20] L. Grcev, "High-frequency grounding," in *Lightning Protection*, IET Power and Energy Series 48, V. Cooray Ed., London, UK: Inst. Eng. Technol., 2010.

[21] D. Cavka, N. Mora, and F. Rachidi, "A comparison of frequency-dependent soil models: Application to the analysis of grounding systems," *IEEE Trans. Electromagn. Compat.*, vol. 56, no. 1, pp. 177–187, Feb. 2014.

[22] CIGRE WG C4.33, "Impact of soil-parameter frequency dependence on the response of grounding electrodes and on the lightning performance of electrical systems," Tech. Brochure 781, Oct. 2019.

[23] A. C. S. de Lima and C. Portela, "Inclusion of frequency-dependent soil parameters in transmission-line modeling," *IEEE Trans. Power Del.*, vol. 22, no. 1, pp. 492–499, Jan. 2007.

[24] M. M. Y. Tomasevich and A. C. S. Lima, "Impact of frequency-dependent soil parameters in the numerical stability of image approximation-based line models," *IEEE Trans. Electromagn. Compat.*, vol. 58, no. 1, pp. 323–326, Feb. 2016.

[25] M. A. O. Schroeder, M. T. C. de Barros, A. C. S. Lima, M. M. Afonso, and R. A. R. Moura, "Evaluation of the impact of different frequency dependent soil models on lightning overvoltages," *Electr. Power Syst. Res.*, vol. 159, pp. 40–49, Jun. 2018.

[26] R. Alipio and S. Visacro, "Frequency dependence of soil parameters: Effect on the lightning response of grounding electrodes," *IEEE Trans. Electromagn. Compat.*, vol. 55, no. 1, pp. 132–139, Feb. 2013.

[27] M. Akbari, K. Sheshyekani, and M. R. Alemi, "The effect of frequency dependence of soil electrical parameters on the lightning performance of grounding systems," *IEEE Trans. Electromagn. Compat.*, vol. 55, no. 4, pp. 739–746, Aug. 2013.

[28] M. Akbari *et al.*, "Evaluation of lightning electromagnetic fields and their induced voltages on overhead lines considering the frequency dependence of soil electrical parameters," *IEEE Trans. Electromagn. Compat.*, vol. 55, no. 6, pp. 1210–1219, Dec. 2013.

[29] K. Sheshyekani and M. Akbari, "Evaluation of lightning-induced voltages on multiconductor overhead lines located above lossy dispersive soil," *IEEE Trans. Power Del.*, vol. 29, no. 2, pp. 683–690, Apr. 2014.

[30] J. Paknahad, K. Sheshyekani, F. Rachidi, M. Paolone, and A. Mimouni, "Evaluation of lightning-induced currents on cables buried in a lossy dispersive ground," *IEEE Trans. Electromagn. Compat.*, vol. 56, no. 6, pp. 1522–1529, Dec. 2014.

[31] A. P. C. Magalhães, J. C. L. V. Silva, A. C. S. Lima, and M. T. C. de Barros, "Validation limits of quasi-TEM approximation for buried bare and insulated cables," *IEEE Trans. Electromagn. Compat.*, vol. 57, no. 6, pp. 1690–1697, Dec. 2015.

[32] T. A. Papadopoulos, Z. G. Datsios, A. I. Chrysochos, P. N. Mikropoulos, and G. K. Papagiannis, "Impact of the frequency-dependent soil electrical properties on the electromagnetic field propagation in underground cables," in *Proc. IPST*, Perpignan, France, Jun. 2019, Art. no. 31.

[33] Z. G. Datsios, P. N. Mikropoulos, and E. T. Staikos, "Methods for field measurement of the frequency-dependent soil electrical properties: Evaluation of electrode arrangements through FEM computations," in *Proc. 21st ISH*, Budapest, Hungary, Aug. 2019, Art. no. 760.

[34] E. F. Vance, *Coupling to Shielded Cables*. Hoboken, NJ, USA: Wiley, 1978.

[35] A. I. Chrysochos, T. A. Papadopoulos, and G. K. Papagiannis, "Robust calculation of frequency-dependent transmission line transformation matrices using the Levenberg-Marquardt method," *IEEE Trans. Power Del.*, vol. 29, no. 4, pp. 1621–1629, Aug. 2014.

[36] A. I. Chrysochos, T. A. Papadopoulos, and G. K. Papagiannis, "Enhancing the frequency-domain calculation of transients in multiconductor power transmission lines," *Elect. Power Syst. Res.*, vol. 122, pp. 56–64, May 2015.

[37] A. I. Chrysochos, T. A. Papadopoulos, and G. K. Papagiannis, "Rigorous calculation method for resonance frequencies in transmission line responses," *IET Gener. Transm. Distrib.*, vol. 9, no. 8, pp. 767–778, May 2015.